

Lattice QCD at finite temperature and chemical potential

Z. Fodor*

*Department of Physics, University of Wuppertal, Germany and
Institute for Theoretical Physics, Eotvos University, Budapest, Hungary
E-mail: fodor@bodri.elte.hu,*

Recent results on finite temperature and/or density lattice QCD are reviewed. Lattice techniques and some previous results are shortly discussed. Results for the critical point at physical quark masses are presented. The equation of state (pressure) and the quark number density are determined at non-vanishing chemical potentials.

*29th Johns Hopkins Workshop on current problems in particle theory: strong matter in the heavens
1-3 August
Budapest*

*Speaker.

1. Introduction

In QCD with increasing temperatures (T) we expect a transition at some $T = T_c$. The dominant degrees of freedom are hadrons in the low temperature phase and colored objects in the high temperature phase. Present lattice results suggest a cross-over for vanishing chemical potential and a critical point at some non-vanishing T and chemical potential (μ).

Since we are mostly interested in the physics around T_c , non-perturbative methods are necessary among which lattice QCD is the most systematic one. There are at least two serious difficulties with lattice simulations. The first one is connected to the lightness of the quark masses. The cost of computations increases strongly as the quark masses decrease, therefore most lattice results were obtained with unphysically large quark masses. The second difficulty is connected to the continuum limit. Calculations are always performed at a finite lattice spacing (a). In order to get physical results, we have to take the $a \rightarrow 0$ limit. Since e.g. for the equation of state (EoS) the computational costs scale as a^{-13} it is not surprising that up to very recently most results were obtained only at one set of lattice spacings.

The situation is much easier in the case of the pure gauge theory. The first problem does not exist since the quark masses are infinite. Due to this situation there are continuum extrapolated results e.g. for the equation of state, both with unimproved and improved lattice actions and they show nice agreement [1, 2, 3].

For a long time it was believed that no physical answer can be given to questions with non-vanishing baryonic densities. The reason for that is the infamous sign problem, which spoils any Monte-Carlo method based on importance sampling. Recently, new techniques were developed, which are able to cover small to moderate baryonic chemical potentials at non-vanishing temperatures (chemical potential is used to set the baryonic density).

In this talk recent results on non-vanishing densities are presented.

2. Lattice formulation, nonvanishing temperatures and densities

Thermodynamical quantities can be obtained from the partition function which can be given by a Euclidean path-integral:

$$Z = \int \mathcal{D}U \mathcal{D}\bar{\Psi} \mathcal{D}\Psi \exp[-S_E(U, \bar{\Psi}, \Psi)] \quad (2.1)$$

where U and $\bar{\Psi}, \Psi$ are the gauge and fermionic fields and S_E is the Euclidean action. The lattice regularization of this action is not unique. There are several possibilities to use improved actions which have the same continuum limit as the unimproved ones. The advantage of improved actions is that the discretization errors are reduced.

Usually S_E can be split up as $S_E = S_g + S_f$ where S_g is the gauge action containing only the self interactions of the gauge fields and S_f is the fermionic part. The gauge action has one parameter, the β gauge coupling, while the parameters of S_f are the m_q quark masses and μ_q chemical potentials. For the fermionic action the two most widely used discretization types are the Wilson and staggered fermions.

For the actual calculations finite lattice sizes of $N_s^3 N_t$ are used. The physical volume and the temperature are related to the lattice extensions as:

$$V = (N_s a)^3, \quad T = \frac{1}{N_t a}. \quad (2.2)$$

Therefore lattices with $N_t \gg N_s$ are referred to as zero temperature lattices while the ones with $N_t < N_s$ are finite temperature lattices. Since the gauge coupling β has the largest influence on the lattice spacing, it essentially determines the temperature (increasing β increases T).

Though QCD at finite chemical potential (μ , which as already mentioned, is used to set non-vanishing baryonic density) can be formulated on the lattice [7], standard Monte-Carlo techniques can not be used at $\mu \neq 0$. The reason is that for non-vanishing real μ the functional measure –thus, the determinant of the Euclidean Dirac operator– is complex. This fact spoils any Monte-Carlo technique based on importance sampling. Several suggestions were studied earlier to solve the problem. Unfortunately, none of them was able to give physical answers for non-vanishing densities. About three years ago new techniques appeared, with which moderate chemical potentials could be reached on the lattice.

One of the most popular ideas [4, 5] was to produce an ensemble of QCD configurations at $\mu=0$ and at the corresponding transition temperature T_c (or at any other physically motivated point for which importance sampling works). Then one determined the Boltzmann weights [8] of these configurations at $\mu \neq 0$ and at T lowered to the transition temperatures at this non-vanishing μ . An ensemble of configurations at a transition point was reweighted to an ensemble of configurations at another transition point.

3. Results with physical quark masses, critical endpoint on the μ -T plane

A critical point is expected in QCD on the temperature versus baryonic chemical potential plane. Our goal in this section is to determine the location of this critical point.

The lattice action we used was the unimproved staggered action with physical quark masses (it means, that the pion and kaon masses take approximately their physical values).

The partition function of lattice QCD with n_f degenerate staggered quarks is given by the functional integral of the gauge action S_g at gauge coupling β over the link variables U , weighted by the determinant of the quark matrix M , which can be rewritten [4] as

$$\begin{aligned} Z(\beta, m, \mu) &= \int \mathcal{D}U \exp[-S_g(\beta, U)] [\det M(m, \mu, U)]^{n_f/4} \\ &= \int \mathcal{D}U \exp[-S_g(\beta_w, U)] [\det M(m_w, \mu_w, U)]^{n_f/4} \\ &\quad \left\{ \exp[-S_g(\beta, U) + S_b(\beta_w, U)] \left[\frac{\det M(m, \mu, U)}{\det M(m_w, \mu_w, U)} \right]^{n_f/4} \right\}, \end{aligned} \quad (3.1)$$

where m is the quark mass, μ is the quark chemical potential and n_f is the number of flavors. For non-degenerate masses one uses simply the product of several quark matrix determinants on the 1/4-th power. Standard importance sampling works and can be used to collect an ensemble of configurations at m_w , β_w and μ_w (with e.g. $\text{Re}(\mu_w)=0$ or non-vanishing isospin chemical potential). It means we treat the terms in the curly bracket as an observable –which is measured on

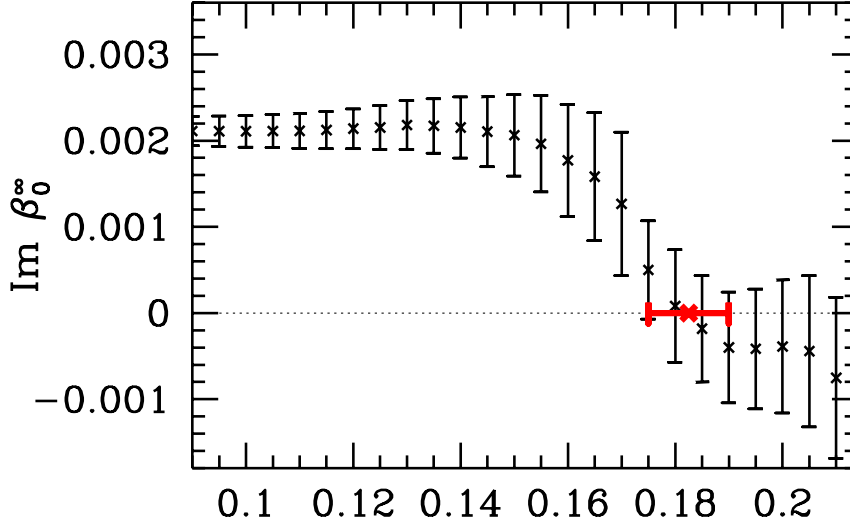


Figure 1: $\text{Im}(\beta_0^\infty)$ as a function of the chemical potential.

each independent configuration— and the rest as the measure. By simultaneously changing several parameters e.g. β and μ one can ensure that even the mismatched measure at β_w and μ_w samples the regions where the original integrand with β and μ is large. In practice the determinant is evaluated at some μ and a Ferrenberg-Swendsen reweighting [8] is performed for the gauge coupling β . The fractional power in eq. (3.1) can be taken by using the fact that at $\mu = \mu_w$ the ratio of the determinants is 1 and the ratio is a continuous function of the chemical potential. The details of the determinant calculation can be found in Ref. [5].

In the following we keep μ real and look for the zeros of the partition function on the complex β plane. These are the Lee-Yang zeros [11]. Their $V \rightarrow \infty$ behavior tells the difference between a crossover and a first order phase transition. At a first order phase transition the free energy $\propto \log Z(\beta)$ is non-analytic. Clearly, a phase transition can appear only in the $V \rightarrow \infty$ limit, but not in a finite V . Nevertheless, the partition function has Lee-Yang zeros at finite V . These are at “unphysical” complex values of the parameters, in our case at complex β -s. For a system with a first order phase transition these zeros approach the real axis in the $V \rightarrow \infty$ limit (the detailed analysis suggests a $1/V$ scaling). This $V \rightarrow \infty$ limit generates the non-analyticity of the free energy. For a system with crossover the free energy is analytic, thus the zeros do not approach the real axis in the $V \rightarrow \infty$ limit.

Figure 1 shows $\text{Im}(\beta_0^\infty)$ as a function of μ enlarged around the endpoint μ_{end} . The picture is simple and reflects the physical expectations. For small μ -s the extrapolated $\text{Im}(\beta_0^\infty)$ is inconsistent with a vanishing value, and the prediction is a crossover. Increasing μ the value of $\text{Im}(\beta_0^\infty)$ decreases, thus the transition becomes consistent with a first order phase transition.

Setting the scale leads to the final results of the analysis. As we already discussed, the quark masses, used to determine the endpoint, correspond approximately to their physical values. The pion to rho mass ratio, extrapolated to our $T \neq 0$ parameters, is 0.188(2) (its physical value is 0.179), whereas the pion to K mass ratio in the same limit is 0.267(1) (its physical value is 0.277).

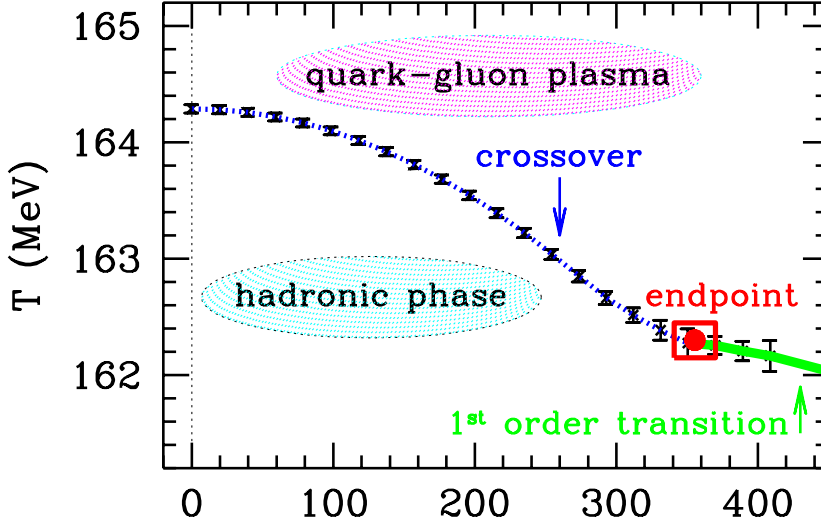


Figure 2: The phase diagram in physical units. Dotted line illustrates the crossover, solid line the first order phase transition. The small square shows the endpoint. The depicted errors originate from the reweighting procedure. Note, that an overall additional error of 1.3% comes from the error of the scale determination at $T=0$. Combining the two sources of uncertainties one obtains $T_E = 162 \pm 2$ MeV and $\mu_E = 360 \pm 40$ MeV.

Figure 2 shows the phase diagram in physical units, thus T as a function of μ_B , the baryonic chemical potential (which is three times larger than the quark chemical potential). At $\mu=0$ the transition between the hadronic and quark-gluon plasma phases is a cross-over. As we increase the chemical potential the transition temperature decreases, but the transition itself remains a cross-over. At a given endpoint chemical potential the transition is a second order one. For even larger chemical potentials the transition temperature further decreases and the transition becomes a first order one.

The curvature of the crossover line separating the QGP and the hadronic phases is given by $T/T_c = 1 - C\mu_B^2/T_c^2$ with $C=0.0032(1)$.

The endpoint is at $T_E = 162 \pm 2$ MeV, $\mu_E = 360 \pm 40$ MeV.

4. Equation of state at non-vanishing T and μ

The equation of state (EOS) at $\mu \neq 0$ is [9] essential to describe the quark gluon plasma (QGP) formation at heavy ion collider experiments.

We use $4 \cdot N_s^3$ lattices at $T \neq 0$ with $N_s=8,10,12$ for reweighting and we extrapolate to $V \rightarrow \infty$ using the available volumes (V). At $T=0$ lattices of $24 \cdot 14^3$ are taken for vacuum subtraction and to connect lattice parameters to physical quantities. 14 different β values are used, which correspond to $T/T_c = 0.8, \dots, 3$. Our $T=0$ simulations provided R_0 and σ . The lattice spacing at T_c is ≈ 0.25 – 0.30 fm. We use 2+1 flavours of dynamical staggered quarks. While varying β (thus T) we keep the physical quark masses approx. constant (the pion to rho mass ratio is $m_\pi/m_\rho \approx 0.66$).

The determination of the equation of state at $\mu \neq 0$ needs several observables, O , at $\mu \neq 0$. This

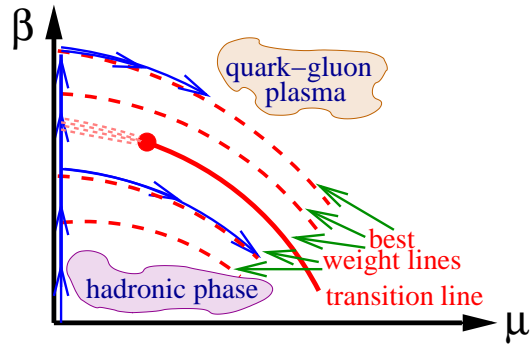


Figure 3: The best weight lines on the μ - β plane. In the middle we indicate the transition line. Its first dotted part is the crossover region. The blob represents the critical endpoint, after which the transition is of first order. The integration paths used to calculate p are shown by the arrows along the β axis and the best weight lines.

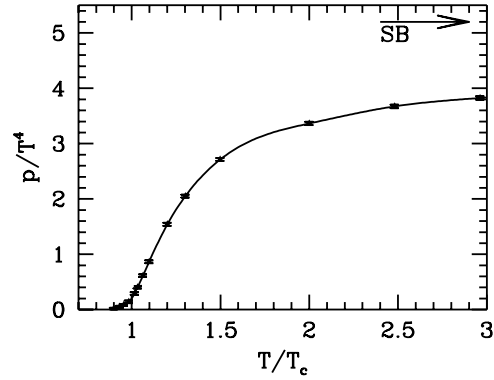


Figure 4: p normalised by T^4 as a function of T/T_c at $\mu = 0$ (to help the continuum interpretation the raw lattice result is multiplied by $c_\mu=0.446$).

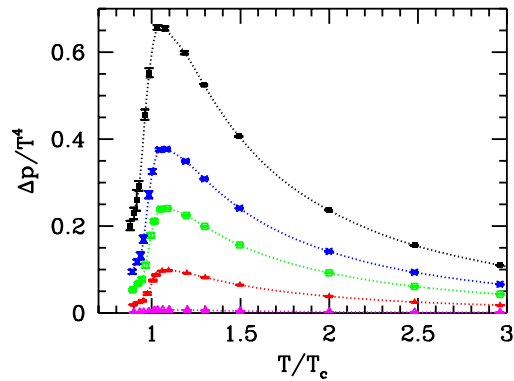


Figure 5: $\Delta p = p(\mu \neq 0, T) - p(\mu = 0, T)$ normalised by T^4 as a function of T/T_c for $\mu_B=100, 210, 330, 410$ MeV and 530 MeV (from bottom to top). To help the continuum interpretation the raw lattice result is multiplied by $c_\mu=0.446$.

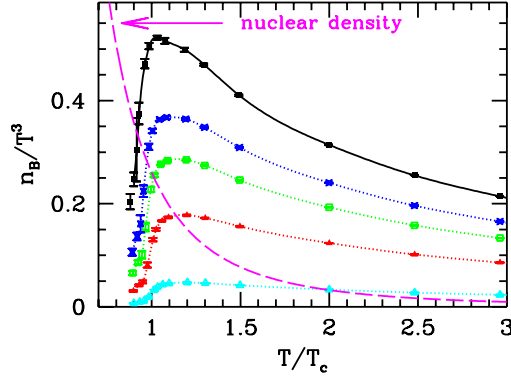


Figure 6: n_B/T^3 versus T/T_c for the same μ_B values as in Fig. 3 (from bottom to top). (to help the continuum interpretation the raw lattice result is multiplied by $c_\mu=0.446$). As a reference value the line starting in the left upper corner indicates the nuclear density.

is obtained by using the weights of eq. (3.1)

$$\overline{O}(\beta, \mu, m) = \frac{\sum\{w(\beta, \mu, m, U)\}O(\beta, \mu, m, U)}{\sum\{w(\beta, \mu, m, U)\}}. \quad (4.1)$$

p can be obtained from the partition function as $p=T \cdot \partial \log Z / \partial V$ which can be written as $p=(T/V) \cdot \log Z$ for large homogeneous systems. On the lattice we can only determine the derivatives of $\log Z$ with respect to the parameters of the action (β, m, μ) . Using the notation $\langle O(\beta, \mu, m) \rangle = \overline{O}(\beta, \mu, m)_{T \neq 0} - \overline{O}(\beta, \mu = 0, m)_{T=0}$. p can be written as an integral:

$$\frac{p}{T^4} = \frac{1}{T^3 V} \int d(\beta, m, \mu) \left(\left\langle \frac{\partial(\log Z)}{\partial \beta} \right\rangle, \left\langle \frac{\partial(\log Z)}{\partial m} \right\rangle, \left\langle \frac{\partial(\log Z)}{\partial \mu} \right\rangle \right). \quad (4.2)$$

The integral is by definition independent of the integration path. The chosen integration paths are shown in Fig 3.

The energy density can be written as $\varepsilon = (T^2/V) \cdot \partial(\log Z) / \partial T + (\mu T/V) \cdot \partial(\log Z) / \partial \mu$. By changing the lattice spacing T and V are simultaneously varied. The special combination $\varepsilon - 3p$ contains only derivatives with respect to a and μ :

$$\frac{\varepsilon - 3p}{T^4} = - \frac{a}{T^3 V} \frac{\partial \log(Z)}{\partial a} \Big|_{\mu} + \frac{\mu}{T^3 V} \frac{\partial \log(Z)}{\partial \mu} \Big|_a. \quad (4.3)$$

The quark number density is $n = (T/V) \cdot \partial \log(Z) / \partial \mu$ which can be measured directly or obtained from p (baryon density is $n_B=n/3$ and baryonic chemical potential is $\mu_B=3\mu$).

We present direct lattice results on $p(\mu = 0, T)$, $\Delta p(\mu, T) = p(\mu \neq 0, T) - p(\mu = 0, T)$ and $n_B(\mu, T)$. Additional overall factors were used to help the phenomenological interpretation.

Fig. 4 shows p at $\mu=0$. In Fig. 5 we show $\Delta p/T^4$ for different μ values. Fig. 6 gives the baryonic density as a function of T/T_c for different μ -s. The densities can exceed the nuclear density by up to an order of magnitude.

5. Summary

We discussed the overlap-improving multi-parameter reweighting technique, in order to calculate physical observables at non-vanishing temperatures and chemical potentials. A critical point is expected in QCD on the temperature versus baryonic chemical potential plane. Using the above lattice method for $\mu \neq 0$ we studied dynamical QCD with $n_f=2+1$ staggered quarks of physical masses on $L_t = 4$ lattices. We used physical quark masses in this analysis. Our result for the critical point is $T_E = 162 \pm 2$ MeV and $\mu_E = 360 \pm 40$ MeV. The continuum limit extrapolation is missing in this case.

The same overlap-improving multi-parameter reweighting technique can be used to determine the equation of state at non-vanishing chemical potentials. Results were presented for the pressure and quark number density as a function of the temperature for different chemical potentials. Note, that the quark mass was in this case larger than its physical value. The continuum limit extrapolation is missing also in this case.

The details of the presented results can be found in [5, 10].

6. Acknowledgments

This work was partially supported by OTKA Hungarian Science Grants No. T34980, T37615, M37071, T032501, AT049652. and by the EU Hadron physics project RII3CT20040506078.

The computations were carried out at Eötvös University on the 330 processor PC cluster of the Institute for Theoretical Physics [12] and the 1024 processor PC cluster of Wuppertal University.

References

- [1] G. Boyd, et al., *Thermodynamics of SU(3) Lattice Gauge Theory*, Nucl. Phys. B **469** (1996) 419 [arXiv:hep-lat/9602007].
- [2] M. Okamoto *et al.*, *Equation of state for pure SU(3) gauge theory with renormalization group improved action*, Phys. Rev. D **60** (1999) 094510 [arXiv:hep-lat/9905005].
- [3] Y. Namekawa *et al.*, *Thermodynamics of SU(3) gauge theory on anisotropic lattices*, Phys. Rev. D **64** (2001) 074507 [arXiv:hep-lat/0105012].
- [4] Z. Fodor and S. D. Katz, *A new method to study lattice QCD at finite temperature and chemical potential*, Phys. Lett. B **534** (2002) 87 [arXiv:hep-lat/0104001].
- [5] Z. Fodor and S. D. Katz, *Lattice determination of the critical point of QCD at finite T and mu*, JHEP **0203** (2002) 014 [arXiv:hep-lat/0106002]; Z. Fodor and S. D. Katz, *Critical point of QCD at finite T and mu, lattice results for physical quark masses*, JHEP **04** (2004) 050 [arXiv:hep-lat/0402006];
- [6] C. R. Allton *et al.*, *The QCD thermal phase transition in the presence of a small chemical potential*, Phys. Rev. D **66** (2002) 074507 [arXiv:hep-lat/0204010]. P. de Forcrand and O. Philipsen, *The QCD phase diagram for small densities from imaginary chemical potential*, Nucl. Phys. B **642** (2002) 290 [arXiv:hep-lat/0205016]. M. D'Elia and M. P. Lombardo, *Finite density QCD via imaginary chemical potential*, Phys. Rev. D **67** (2003) 014505 [arXiv:hep-lat/0209146]. A. Alexandru, M. Faber, I. Horvath and K. F. Liu, *Lattice QCD at finite density via a new canonical approach*, Phys. Rev. D **72** (2005) 114513 [arXiv:hep-lat/0507020]. V. Azcoiti, G. Di Carlo, A. Galante and V. Laliena, *Phase diagram of QCD with four quark flavors at finite temperature and baryon density*, Nucl. Phys. B **723**

- (2005) 77 [arXiv:hep-lat/0503010]. R. V. Gavai and S. Gupta, *Pressure and non-linear susceptibilities in QCD at finite chemical potentials*, Phys. Rev. D **68** (2003) 034506 [arXiv:hep-lat/0303013].
- C. R. Allton, et al., *The equation of state for two flavor QCD at non-zero chemical potential*, Phys. Rev. D **68** (2003) 014507 [arXiv:hep-lat/0305007].
- [7] P. Hasenfratz and F. Karsch, *Chemical Potential On The Lattice*, Phys. Lett. B **125** (1983) 308; J. B. Kogut, H. Matsuoka, M. Stone, H. W. Wyld, S. H. Shenker, J. Shigemitsu and D. K. Sinclair, *Chiral Symmetry Restoration In Baryon Rich Environments*, Nucl. Phys. B **225** (1983) 93.
- [8] A. M. Ferrenberg and R. H. Swendsen, *New Monte Carlo Technique For Studying Phase Transitions*, Phys. Rev. Lett. **61** (1988) 2635; A. M. Ferrenberg and R. H. Swendsen, *Optimized Monte Carlo Analysis*, Phys. Rev. Lett. **63** (1989) 1195.
- [9] Z. Fodor, S. D. Katz and K. K. Szabo, *The QCD equation of state at nonzero densities: Lattice result*, Phys. Lett. B **568** (2003) 73 [arXiv:hep-lat/0208078].
- [10] F. Csikor, et al., *Equation of state at finite temperature and chemical potential, lattice QCD results*, JHEP **0405** (2004) 046 [arXiv:hep-lat/0401016].
- [11] C. N. Yang and T. D. Lee, *Statistical Theory Of Equations Of State And Phase Transitions. 1. Theory Of Condensation*, Phys. Rev. **87** (1952) 404; T. D. Lee and C. N. Yang, *Statistical Theory Of Equations Of State And Phase Transitions. 2. Lattice Gas And Ising Model*, Phys. Rev. **87** (1952) 410.
- [12] Z. Fodor, S. D. Katz and G. Papp, *Better than \$1/Mflops sustained: A scalable PC-based parallel computer for lattice QCD*, Comput. Phys. Commun. **152** (2003) 121 [arXiv:hep-lat/0202030].